International Journal of Electrical Electronics & Computer Science Engineering
Volume 4, Issue 6 (December, 2017) | E-ISSN : 2348-2273 | P-ISSN : 2454-1222
Available Online at www.ijeecse.com

A Multi-Port Half Bridge DC-DC Converter for PV Application

Faheem Khan[2], Mini Rajeev[1]
Department of Electrical Engineering, Fr. C. Rodrigues Institute of Technology, Vashi, Navi Mumbai
faheemkhan@live.in,minirajeev1@yahoo.co.in

Abstract: ***This paper discusses a multiport converter which consists of a single power processing stage with multiple input ports and single output port. Here, solar energy is considered as the main source and battery as the energy storage device. The system comprises of a Photovoltaic panel, lead acid battery, triple port half bridge dc to dc converter, control circuit and the load.Simulation results of the system with synchronous regulation are discussed for low voltage application. To validate the simulation results, a laboratory prototype was developedand tested using Digital Signal Controller TMS320F28069.The experimentalresults show that the performance of the converter is as expected.***

Keywords: Half bridge converter, PV, Triple port converter, DSP.

I. INTRODUCTION

Renewable energy resources are getting more attention in a broad range of applications, and hence there is a supreme need for power converters that are capable of interfacing, and simultaneously controlling several power terminals with low cost, high efficiency and compact structure [1]. The use of some kind of energy storage system is a must in most of the applications that uses renewable sources. A multiport interface is quite useful for such systems that require storage in addition to the main source. Power electronic converters are also necessary for interfacing, as the voltage level and the voltage - current characteristics of the energy source and storage elements are different from those of the loads.

In the conventional structure with multiple power sources, the power electronics interface is realized by connecting separate dc-dc converters.Those converters are linked through a common dc bus but usually they are controlled separately. Here the drawbacks are high cost, high component count and low efficiency due to multiple-stage power conversion. However, the use of integrated power converter as shown in Fig.1[3], which is defined as multi-port converter. The advantages of multiport converters are reduced cost due to less component count and associated circuits, higher power density, efficient thermal management, improved reliability because of compact layout and easier implementation of centralized control**.**Several multiport converter topologies have been recently reported in the literature.

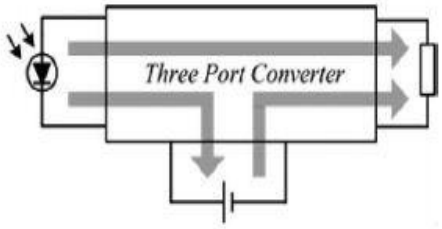

Fig. 1. Multiport Port converter

The reported multiport topologies for integrating different power sources are three port triple full bridge converter, three port triple half bridge converter,integrated three port full bridge converters,integrated three port half bridge converter etc. Among them, one simple method is to interface several converter stages to a common dc bus [8**]**. Other integratedtriple port converters(TPC) are configured from half-bridgeconverter (HBC) or full-bridgeconverter (FBC) topology with magnetic coupling via a high-frequency transformer [2]. But these converters utilize many switches, resulting in complicated driving and control circuitry, and may degrade the performance of integrated converters.TPC with half bridge topology (TPHBC) has the several advantages such as cost effectiveness, reduction in losses and ease of control compared to other topologies. Hence the preferred topology for low power application is TPHBC with synchronous regulation (THBC-SR).

This paper presents TPHBC-SR with PV as the main source. As solar energy is uncertain, battery is used to compensate for the mismatch between source and load power.Simulation and hardware results are presented in this paper.

II. TPHBC-SR

In a TPC built from an HBCas shown in Fig.2[3], ifa storage element such as battery is connected in parallel with the input capacitor of the HBC, the battery can either be charged or discharged by controlling the main switches of the HBC. A triple port converter(TPC) is derived by configuring three power flow paths, in which a single-stage power conversion is achieved between any two of these three ports.

International Journal of Electrical Electronics & Computer Science Engineering
Volume 4, Issue 6 (December, 2017) | E-ISSN : 2348-2273 | P-ISSN : 2454-1222
Available Online at www.ijeecse.com

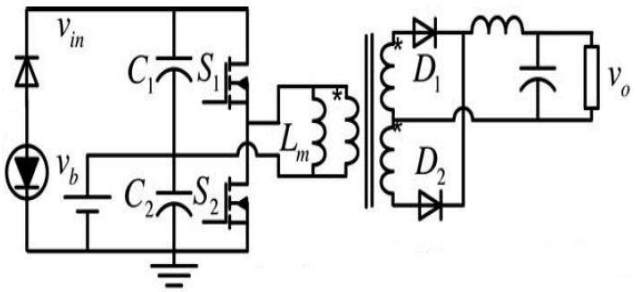

Fig. 2. TPHBC

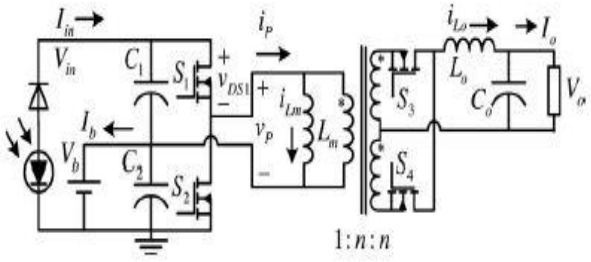

Fig. 3. TPHBC-SR

As for a TPC, the output port usually has to be tightly regulated to meet the load requirements, while the input port from a renewable source like PV should be implemented using maximum power tracking. The storage element should be bidirectional to balance the power mismatch between input power and the load. This means that two of the three ports should be controlled independently and the third one is used for power balance. As a result, two independent variables are necessary to be controlled. To achieve two independent ports controllable, we can do a modification in the TPHBC topology from any of the three aspects [3] given below.

1) TPHBC with Post regulation: Post regulation is employed to achieve output voltage control while maintaining the two primary switches S_1 and S_2 driven in complement.

2) TPHBC with Synchronous Regulation: S_1 and S_2 are operated as the two independent switches while a freewheeling route for themagnetizing inductor $L_m$is whenS_1 and $S_2$are OFF is through MOSFETs replacing the diodes in the secondary circuit.

3) TPHBC with Primary Freewheeling: S_1 and S_2 are operated independently while an additional freewheeling branch in the primary for L_m is introduced.

The two primary switches $S_1$and S_2 from Fig.3 are driven with duty cycle D_1 and D_2. The synchronous rectifier MOSFETS S_3 and S_4 are driven in complementary with S_2 and S_1, respectively. Therefore, both S_3 and S_4 are ON, when S_1 and S_2 are OFF .This complementary switching shorts the secondary windings of the transformer and build a freewheeling route for the current through the magnetizing inductor L_m.

The TPHBC-SR shown in the Fig.3 has three possible work states: 1) dual-output (DO) state, with $P_{in} > P_o$,the battery absorbs the surplus solar power and both the load and battery take power from PV; 2) dual-input (DI) state, with $P_{in} < P_o$and $P_{in} > 0$, the battery discharges to feed the load along with the PV; and 3) single-input single output (SISO) state,with $P_{in} = 0$, battery supplies the load power alone. P_{in}, P_b, P_o, are the power flows through the PV, battery, and load port. Ignoring the power loss in the conversion, we have [3],

$$P_{in} = P_b + P_O \quad (1)$$

$$V_{in}I_{in} = V_bI_b + V_oI_o \quad (2)$$

Where V_{in}, V_b, V_O are the source, battery and the output voltages and I_{in}, I_b, I_o are the source, battery and the output currents respectively.

III. DESIGN CONSIDERATION

A. Design of High Frequency Transformer

Applying the volt-second balance principle on the magnetizing inductor of the transformer $L_m$and the output filter inductor L_o, we get [3],

$$V_o = 2nD_2V_b \quad (3)$$

$$V_{in} = \frac{(D_1 + D_2)V_b}{D_1} \quad (4)$$

Here 'n' is the transformation ratio.It is assumed thatvoltages of the three ports, V_{in}, V_b, and V_o are constant during the steady state.

B. Design of Inductor and Capacitor:

The output inductor and the capacitor are designed using (5) and (6) respectively [4].

$$L = \frac{DT_s}{\Delta I_L}\left[\frac{n_2V_{dc}}{n_12} - V_0\right] \quad (5)$$

$$C = \frac{DT_s^2}{16L\Delta V_0}\left[\frac{n_2V_{dc}}{n_12} - V_0\right] \quad (6)$$

Where, ΔI_L is the inductor current ripple, V_{dc} is supply voltage, n_1 and n_2 are number of turns on the primary and secondary side of the transformer, V_O is output voltage and T_S is switching time period.

C. Selection of the Switches:

For synchronous regulation, the diodes on the secondary side of the transformer are replaced with MOSFET

International Journal of Electrical Electronics & Computer Science Engineering
Volume 4, Issue 6 (December, 2017) | E-ISSN : 2348-2273 | P-ISSN : 2454-1222
Available Online at www.ijeecse.com

switches. MOSFET switches are used since the selected frequency is 40 KHz and is a low voltage application.

D. Specification of Battery:

The battery selected here is a sealed lead acid battery 6V, 4.5Ah. It charges in the DO mode through power coming from PV panel and it discharges to meet the load in SISO mode. The half bridge converter here has both buck and boost operation. A 6V battery is selected so that the converter will work as boost converter in SISO mode.

E. Specification of PV:

For the input a 50 watt 12V PV panel is considered, since the converter is designed for low power application. The specification of the panel is shown in Table.1.The design parameters considered for simulation as well as for hardware implementation are shown in Table. 2.

Table 1. PV Panel Specification

Maximum power (P_{MAX})	Voltage at P_{MAX} (V_{MP})	Current at P_{MAX} (I_{MP})	Open circuit voltage (V_{OC})	Open circuit current (I_{OC})
50watt	17.4V	2.87A	21.5V	3.18A

Table 2. Design Parameters

	Parameters	Values
Input Voltage	V_{in}	12 to 18V
Battery	V_b	6V
Output	C_o	1.3 µF
Output	L_o	1.2 mH
Output Current	I_o	1A
Output Power	P_o	18 watts
Transformer	N	1:5:5
Switching freq	f_s	40KHz

IV. SIMULATION RESULTS

The entire system was simulated in MATLAB environment. A resistive load of 12Ω is used in this configuration. Mat lab model of closed loop system is shown in Fig.4.Here a 12V,50Wp PV panel, panel at 25^0C with 1sun intensity is used as the input to the system, having V_{oc} of 21.6Vand I_{sc} of 3.26A and maximum power voltage and current as 18.20V, 2.75A.

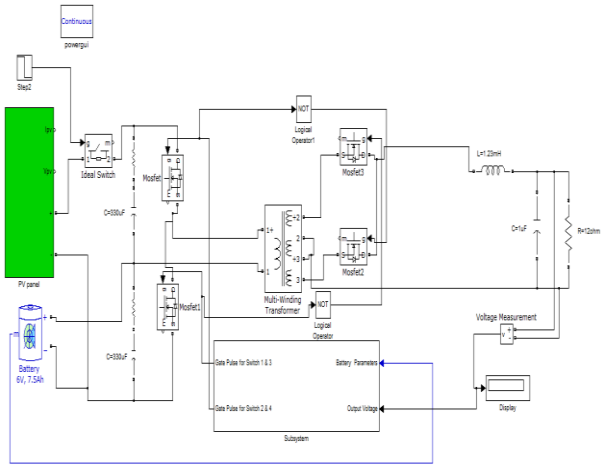

Fig. 4. Model of Closed Loop System

The control of the whole system is done by using two PI controllers as shown in Fig.4. One PI controller is used for the output voltage regulation and the 2nd PI controller is for the battery voltage regulation. The output voltage of the TPHBC-SR is compared with the reference voltage. The error generated is passed through the PI controller. The output of the PI controller controls the duty ratio of the switch S_2. The error is compared with the saw tooth wave of 40 kHz to generate pulses for the switches S_2 and S_3.The duty ratio for switch S_3 is the complement of switch S_2.

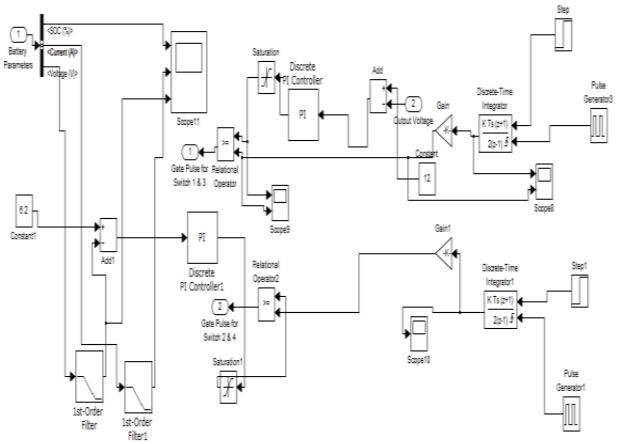

Fig. 5. Control Circuit

International Journal of Electrical Electronics & Computer Science Engineering
Volume 4, Issue 6 (December, 2017) | E-ISSN : 2348-2273 | P-ISSN : 2454-1222
Available Online at www.ijeecse.com

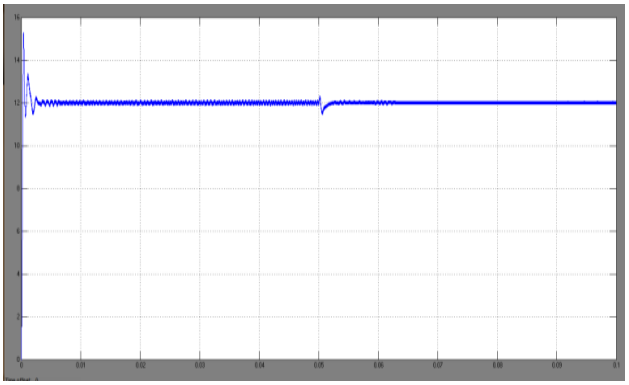

Fig. 6. Output Voltage

The battery voltage is also compared with the reference voltage. The error generated is passed through the second PI controller. The error is compared with similar saw tooth wave to generate pulses for the switches S_1 and S_4. The duty ratio of the switch S_4 is complement of switch S_1.To avoid shoot though between switches duty ratio is limited at 0.45 for each all switches. The output voltage is shown in Fig.6.

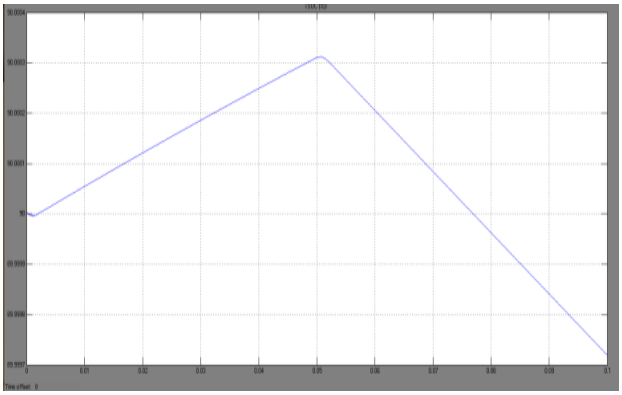

Fig. 7. State of Charge of the Battery

For the first 5ms the PV panel output is supplying power to the load and also for charging the battery. At 5msec, the ideal switch seen in the model in Fig.4 opens up, disconnecting the PV panel from the system. This is done to simulate the conditions of non-availability of sunlight such as in the night or cloudy days. The small surge seen in Fig.6 in the output voltage at 5msec is due to this reason. From 5msec, power is fed to the load by the battery as shown in Fig. 7.

With the same input conditions when output voltage reference was changed to 16V from 12V a regulated output voltage was achieved depending upon the reference voltage as shown in Fig.8. Thus the tuning of PI controller was achieved.

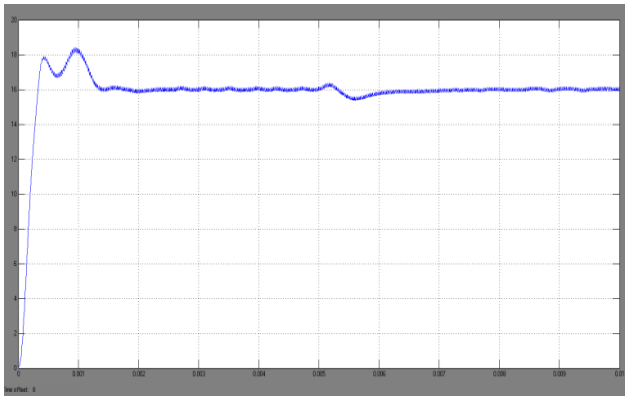

Fig. 8. Output Voltage at 16V

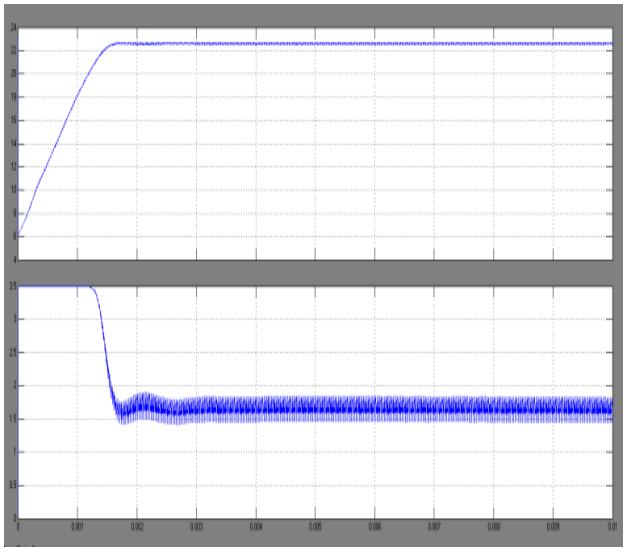

Fig. 9. Output Voltage With Different Input Conditions

When the input was changed i.e. for experimental purpose the intensity of the sun was increased along with the increase temperature as shown in Fig.9, the output voltage was found to be same as the reference voltage. The results show that a regulated output voltage is obtained at the load side, in spite of variations in the input conditions of the PV panel.

V. HARDWARE RESULTS

Hardware implementation of the system is done to validate the simulation results.The controller used is F2000 Piccolo series Digital Signal Controller TMS320F28069 from Texas Instruments. The photo of the TPHBC-SR converter is shown in Fig.10.The sensing circuit board is shown in Fig.11, current sensing is done by LEM current sensor.Voltage is sensed by voltage divider circuit. All the components required for the hardware implementation and testing are tabulated in Table.3.

International Journal of Electrical Electronics & Computer Science Engineering
Volume 4, Issue 6 (December, 2017) | E-ISSN : 2348-2273 | P-ISSN : 2454-1222
Available Online at www.ijeecse.com

Table 3. Components used for Implementation

S.N.	Component	Qty.	Type
1	Switches	4	MOSFET-SPW35N60C3, MOSFET-SPW20N60C3
2	Gate Driver	4	IC-HCPL3120
3	Buffer IC	1	IC-74LS573
4	Rectifier	5	DB107
5	Voltage Regulator	5	LM-7815, LM-7805,
6.	DC Link Capacitor	2	330µF/250V

The Texas Instrument's C2000 Piccolo series Digital Signal Controllers (DSC) is rich in on chip peripherals and has many features making it suitable for power electronics applications. IC HCPL-3120 is selected to drive the MOSFETS.The buffer IC used for interface between the DSP controller and gate driver. The photograph of the complete hardware set up of the converter along with the associated driver circuits of the MOSFET is shown in Fig.10. DSP TMS320F28069 is the main controller of the system.

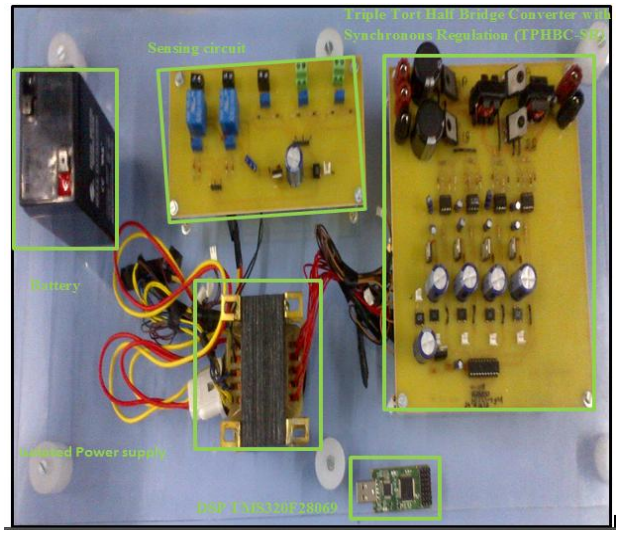

Fig. 10. Complete Hardware Setup

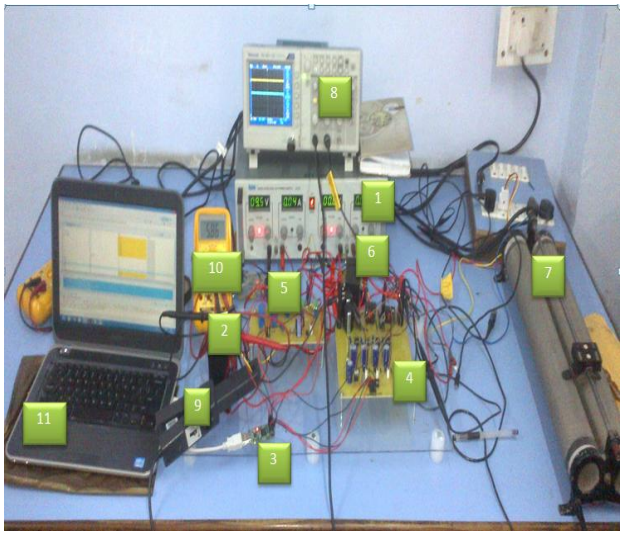

Fig. 11 Laboratory Setup With All the Measuring and Testing Equipment

The laboratory setup consisting of the TPHBC-SR, its driver circuit, the sensing circuit with the two LEM current sensors and three voltage sensors and its auxiliary power supply is shown in Fig 11.For the implementation a dc power supply is used as the main source.

PWM pulses are generated with help of DSP (TMS320F28069). Fig.12 and Fig.13 shows PWM pulses given to switch S_1 & switch S_2 on the primary side of the converter. Here the duty cycle for both the switch was kept at 45%.

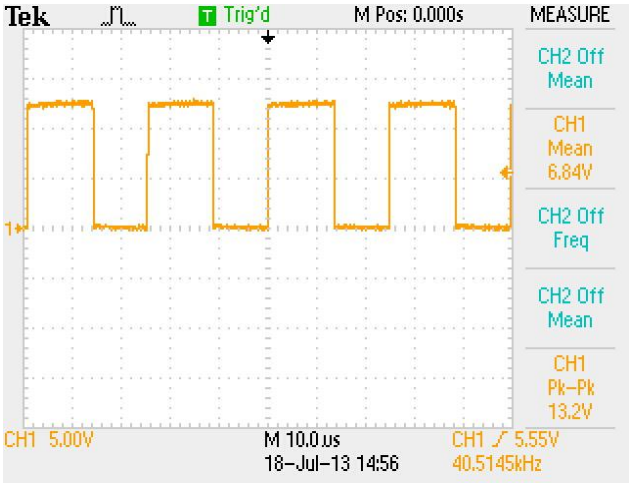

Fig. 12. PWM Pulse of Switch S_1

International Journal of Electrical Electronics & Computer Science Engineering
Volume 4, Issue 6 (December, 2017) | E-ISSN : 2348-2273 | P-ISSN : 2454-1222
Available Online at www.ijeecse.com

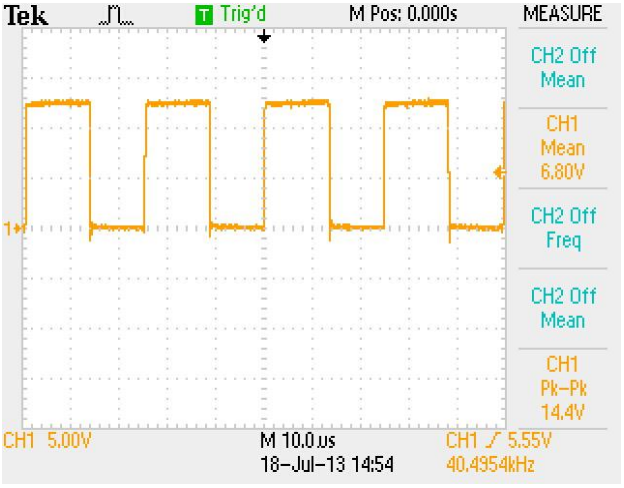

Fig. 13. PWM Pulse of Switch S_2

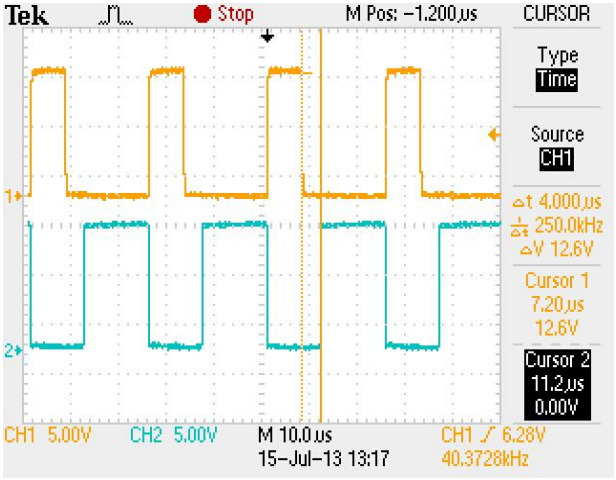

Fig. 14. PWM Pulse of Switch S_1 and Switch S_2 with Dead Band

To avoid shoot through a dead band is given between PWM Pulses for S_1 and S_2 as shown in Fig.15.For testing the circuit, DC voltage source of 13V was connected on the input port, battery of 6V at the bidirectional port and resistive load were also connected at the output port of the converter. The regulated output voltage waveforms of the converter during two modes of operation such as DO and DI modes are shown in Fig.15 and Fig.16 respectively. The waveform seen in orange colour in Fig.15 is the battery current. The negative sign indicates that the current is flowing into the battery; hence it is in charging mode. The charging rate of battery will vary depending on the power coming from the input source and the required output voltage.

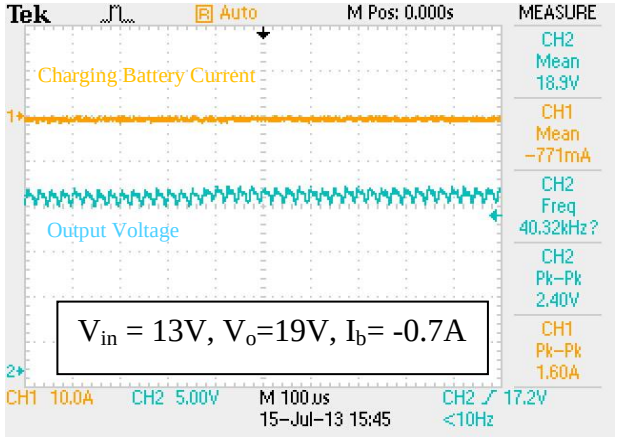

Fig. 15. TPHBC Operating in DO Mode

If the PV is providing the required power then the battery will charge at a high rate and vice versa. This results show that the converter was working in DO mode (dual output mode) as it is charging the battery along with providing power to the load. As seen in Fig.16, when the V_{ref} is keep as 18V, the input voltage was 10.5V hence to meet the load requirement the battery is discharging and the battery current is 0.9A. The actual peak to peak output voltage ripple is 8.8% .Here the rate of battery discharge is low since the input source is also active in the system. The results show that the converter is working in DI mode (dual input mode). In this mode the energy source discharges when input source is at low intensity, together they meet the load requirement.

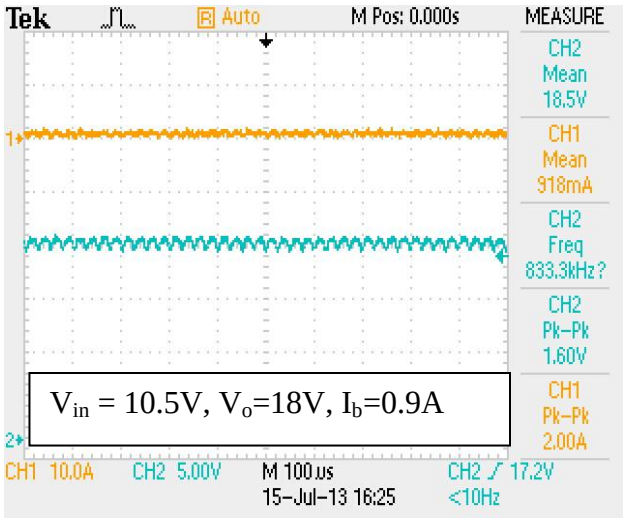

Fig. 16. TPHBC Operating in DI Mode

Now for the third mode SISO (single input single output mode), happens when the source input is inactive. At that time the battery will discharge to maintain the output requirement of the load. In this mode the main input source was deactivated from the circuit and battery acts as

International Journal of Electrical Electronics & Computer Science Engineering
Volume 4, Issue 6 (December, 2017) | E-ISSN : 2348-2273 | P-ISSN : 2454-1222
Available Online at www.ijeecse.com

the input source. Fig.17 shows the measured battery current from the sensing circuit and Fig.18 shows the output voltage waveform during SISO mode. Here the V_{ref} is 16V the battery discharge current is 1.3A and the battery voltage is 5.25V.

Fig. 17. Battery current

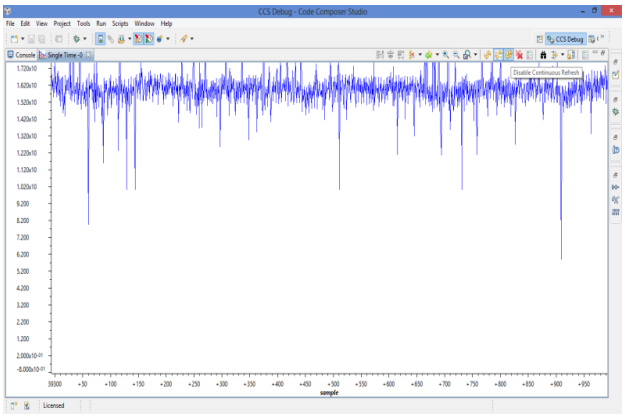

Fig. 18. Observed Output Voltage in SISO

Experimental results are comparable with the simulation results. Spikes are observed in the output voltages. A snubber circuit design needs done to reduce the voltage spikes.

VI. CONCLUSION

This paper has presented the design, simulation and hardware implementation of an integrated three port half bridge dc-dc converter for low power application.Hardware implementation was carried out using Texas Instrument's TMS320F28069, a low cost digital signal controller. A PWM control is applied to the converter interfacing the energy storage to handle voltage variations of the input by adjusting the duty cycle. In this particular converter both buck and boost operation are achieved. The power electronic system shows a complete interface between source, storage element and load and also gives regulated output. Multiport converter has large potential in future applications when interfacing of more than one source is essential.

VII. REFERENCES

[1] Ned Mohan, Power Electronics and Drives 2003 Mnpere Publication.

[2] F. Blaabjerg, Z. Chen, and S. Kjaer, "Power electronics as efficient inter- face in dispersed power generation systems," IEEE Trans. Power Electron., vol. 19, no. 5, pp. 1184–1194, Sep. 2004.

[3] Hongfei Wu, Runruo Chen Junjun Zhang Yan Xing, Haibing Hu, and HongjuanGe. "A Family of Three-Port Half-Bridge Converters for a Stand-Alone Renewable Power System," IEEE Transactions On Power Electronics, Vol. 26, No. 9, September 2011.

[4] L.Umananad, S.R.Bhat "Design of Magnetic Components for Switched Mode Power Converters".

[5] H. Matsuo, W. Lin, F. Kurokawa, T. Shigemizu, and N. Watanabe, "Charac- teristic of the multiple input DC-DC converter," IEEE Trans. Ind. Electron., vol. 51, no. 3, pp. 625–631, Jun. 2004.

[6] A. D. Napoli, F. Crescimbini, S. Rodo, and L. Solero, "Multiple input DC- DC power converter for fuel-cell powered hybrid vehicles," in Proc. IEEE 33rd Power Electronics Specialists Conference (PESC'02), Cairns, Jun. 2002, pp. 1685–1690.

[7] M. Michon, J. L. Duarte, M. Hendrix, and M. G. Simoes, "A three-port bi-directional converter for hybrid fuel cell systems," in Proc. IEEE Power Electronics Specialists Conference (PESC'04), Aachen, Germany, Jun. 2004, pp. 4736–4742.

[8] Y. M. Chen, Y. C. Liu, and F. Y. Wu,"Multi-input DC/DC converter based on the multiwinding transformer for renewable energy applications," IEEE Trans. Ind. Appl., vol. 38, no. 4, pp. 1096–1104, Jul./Aug. 2002.

[9] L. Solero, F. Caricchi, F. Crescimbini, O. Honorati, and F. Mezzetti, "Perfor- mance of a 10 kW power electronic interface for combined wind/PV isolated generating systems," in Proc. IEEE Power Electronics Specialists Conference (PESC'96), Jun. 1996, pp. 1027–1032.

[10] M. Marchesoni and C. Vacca, "New DC-DC converter or energy storage system interfacing in

fuel cell hybrid electric vehicles," IEEE Trans. Power Electron., vol. 22, no. 1, pp. 301–308, Jan. 2007

[11] H. Tao, A. Kotsopoulos, J. L. Duarte, and M. A. M. Hendrix, "Family of multiport bidirectional DC-DC converters," IEE Proceeding Electric Power Applications, vol. 153, no. 3, pp. 451–458, May 2006.

[12] Comparison of Photovoltaic array maximum power point tracking technique - Patrick L Chapman, TrishanEsram.

[13] Study of maximum power point tracking (mppt) techniques in a solar photovoltaic array Department of Electrical Engineering National Institute of Technology Orissa – Arjav.H.

[14] GW. Jiang and B. Fahimi. "Design, Multi-port power electric interface for renewable energy sources," in Proc. IEEE Appl. Power Electron. Conf., Feb. 2009.

[15] A. Hussam, F. Tian, and I. Batarseh, "Tri-modal half-bridge converter topology for three-port interface," IEEE Trans. Power Electron., vol. 22, no. 1, pp. 341–345, Jan. 2007.

[16] TMS320x2806x Technical Reference Guide, Texas Instruments, LiteratureNumber:SPRUH18C,Dec.2011, http://www.ti.com/lt/ug/spruh18c/spruh18c.pdf.

17] S. Chandrasekaran and L. Gokdere, "Integrated magnetics for interleaved DC-DC boost converter for fuel cell powered vehicles," in Proc. IEEE Power Electronics Specialists Conference (PESC'04), Aachen, Germany, Jun. 2004, pp. 356–361.

[18] K. Wang, L. Zhu, D. Qu, H. Odendaal, J. Lai, and F. Lee, "Design, implementation, and experimental results of bidirectional full-bridge DC-DC converter with unified soft-switching scheme and soft-starting capability," in Proc. IEEE Power Electronics Specialists Conference (PESC'00), Jun. 2000, pp. 1058–1063.

[19] M. Jain, M. Daniele, and P. K. Jain, "A bidirectional DC-DC converter topology for low power application," IEEE Trans. Power Electron., vol. 15, no. 4, pp. 595–606, Jul. 2000

[20] M. Marchesoni and C. Vacca, "New DC-DC converter for energy storage system interfacing in fuel cell hybrid electric vehicles," IEEE Trans. Power Electron., vol. 22, no. 1, pp. 301–308, Jan. 2007.